

Realignment of signal processing within a sensory brainstem nucleus as brain temperature declines in the Syrian hamster, a hibernating species

Shin-Ichi Sekizawa · John M. Horowitz ·
Barbara A. Horowitz · Chao-Yin Chen

Received: 9 July 2011 / Revised: 28 November 2011 / Accepted: 13 December 2011 / Published online: 20 January 2012
© Springer-Verlag 2012

Abstract Crucial for survival, the central nervous system must reliably process sensory information over all stages of a hibernation bout to ensure homeostatic regulation is maintained and well-matched to dramatically altered behavioral states. Comparing neural responses in the nucleus tractus solitarius of rats and euthermic Syrian hamsters, we tested the hypothesis that hamster neurons have adaptations sustaining signal processing while conserving energy. Using patch-clamp techniques, we classified second-order neurons in the nucleus as rapid-onset or delayed-onset spiking phenotypes based on their spiking onset to a depolarizing pulse (following a -80 mV prepulse). As temperature decreased from 33 to 15°C, the excitability of all neurons decreased. However, hamster rapid-onset spiking neurons had the highest spiking response and shortest action potential width at every temperature, while hamster delayed-onset spiking neurons had the most negative resting membrane potential. The frequency of spontaneous excitatory postsynaptic currents in both phenotypes decreased as temperature decreased, yet the amplitudes of tractus solitarius stimulation-evoked currents were greater in hamsters than in rats regardless of phenotype and temperature. Changes were significant ($P < 0.05$), supporting our hypothesis by showing that, as

temperature falls, rapid-onset neurons contribute more to signal processing but less to energy conservation than do delayed-onset neurons.

Keywords Nucleus tractus solitarius · Baroreflex · Whole-cell patch-clamp · Second-order neurons

Abbreviations

aCSF	Artificial cerebrospinal fluid
AP	Action potential
CNS	Central nervous system
DS	Delayed-onset spiking
EPSC	Excitatory postsynaptic current
NTS	Nucleus tractus solitarius
RS	Rapid-onset spiking
TS	Tractus solitarius

Introduction

Hibernating species have evolved central nervous system (CNS) adaptations that translate relevant sensory stimuli into signals processed by subcortical structures and enable the animal to survive and thrive in cold environments where food is scarce (Heller 1979; Carey et al. 2003). Thus, even in the deepest stages of a hibernation bout, loud sounds, prodding, or abrupt changes in ambient temperature (i.e., “alarm signals”) can arouse the animal (Heller 1979; Horowitz and Horrigan 1996). Additionally, during entrance into and during torpor, the CNS must continuously and reliably process sensory signals from the internal environment and send appropriate outputs to a variety of effectors (Carey et al. 2003). Brainstem processing of sensory signals at the low body temperatures encountered by mammalian hibernators is further delineated in this study.

Electronic supplementary material The online version of this article (doi:10.1007/s00359-011-0706-x) contains supplementary material, which is available to authorized users.

S.-I. Sekizawa · C.-Y. Chen (✉)
Department of Pharmacology, University of California Davis,
GBSF 3617, 451 Health Sciences Drive, Davis, CA 95616, USA
e-mail: cych@ucdavis.edu

J. M. Horowitz · B. A. Horowitz
Department of Neurobiology, Physiology, and Behavior,
University of California Davis, Davis, CA 95616, USA

Although essential central processing is well maintained over a hibernation bout, in deep hibernation, electrical activity is markedly reduced throughout the whole brain (Heller 1979; Horowitz and Horrigan 1996). As animals enter hibernation, cortical electroencephalography records become flattened, reflecting a loss of synchronized activity (Chatfield and Lyman 1954; Mihailovic 1972; Heller 1979; Horowitz and Horrigan 1996), and 2-deoxyglucose measurements indicate that activity is greatly attenuated in all brain regions (Kilduff et al. 1982, 1990). However, while all neurons reduce their firing rates as brain temperature declines, there may be further realignment of signal processing within each brainstem nucleus, and some neurons may retain a significantly higher level of activity than others, taking on a dominant functional role during hibernation. Alternatively, the activity of all neurons in a brainstem nucleus may be similarly reduced at decreased temperatures, resulting in neural network processing in the hibernating animal that is simply a muted version of that seen in the euthermic animal. To resolve these two alternatives, this study focused on the effects of temperature on the excitability of specific nucleus tractus solitarius (NTS) neuron phenotypes.

The NTS is the first brainstem nucleus that receives and integrates sensory information from the internal environment, including peripheral cardiovascular and pulmonary signals. These signals are transmitted over afferent first-order sensory neurons converging in the tractus solitarius (TS) that enter the NTS and synapse on second-order neurons. Second-order NTS neurons play a pivotal role in homeostatic regulation because signal conditioning at these “gateway” neurons determines the magnitude, pattern, and duration of cardiovascular and respiratory reflex signals transmitted to other brainstem and central sites (Taylor et al. 1999). With a paired-shock protocol, second-order neurons can be identified (Miles 1986; Scheuer et al. 1996; Sekizawa et al. 2003), and a subset of these neurons can be further classified as receiving baroreceptor inputs using fluorescent labeling (Chen et al. 2009; Sekizawa et al. 2009). Recent studies demonstrated that these second-order neurons can undergo both synaptic and intrinsic plasticity, which is important in adaptive changes in neural control of reflex functions (Bonham et al. 2006; Joad et al. 2007). Thus, the first objective of this study was to determine if signal processing mechanisms of second-order NTS neurons in hibernators, including those that receive baroreceptor inputs, exhibit adaptations to sustain signal processing at cold temperatures.

Studies from nonhibernators showed that these second-order NTS neurons can be divided into two distinct phenotypes based on the delay in spiking behavior during injection of a depolarizing current [i.e., a rapid-onset spiking phenotype (RS) with a delay <20 ms between the

onset of depolarization and the first spike, and a delayed-onset spiking phenotype (DS) with a delay >100 ms]. These two phenotypes in the NTS adapt differently to air pollution exposure (Sekizawa et al. 2010b), have different amplitudes of transient outward potassium current (Sekizawa et al. 2010a), and exhibit different sensitivities to 4-aminopyridine (Bailey et al. 2002). Thus, a second objective of this study was to determine if neural properties of hamster RS and DS phenotypes have identical types and degrees of adaptation or alternatively, if each phenotype has a distinct set of adaptations that alters its function at low temperatures.

Combining data on both intrinsic (non-synaptic) and synaptic properties allows overall delineation of the role of each hamster NTS phenotype in terms of alterations in its signal processing as temperature declines. To describe this plasticity in phenotypic roles, we tested the following two hypotheses: (1) intrinsic properties of rat and hamster NTS phenotypes differ at euthermic temperatures, with additional species differences becoming apparent as temperature is lowered, and (2) synaptic properties of rat and hamster NTS differ at euthermic temperatures, with additional differences becoming apparent as temperature is lowered.

Methods

Brainstem slice preparation, bath temperature control, and electrophysiology

Male adult euthermic Syrian hamsters (*Mesocricetus auratus*; $n = 9$; 129 ± 3 g) from our UC Davis hamster colony were bred from animals selected over generations to more readily hibernate. Male adult Sprague Dawley rats ($n = 7$; 457 ± 10 g; from Charles River, Wilmington, MA, USA) were chosen as a nonhibernating mammalian control. Sprague Dawley rats were 14–15 weeks old (i.e., 3.5–3.75 months of age), and Syrian hamsters were 18–56 weeks (4.5–14 months) old, and thus old enough to hibernate. Animals were decapitated, and the brain was rapidly submerged in ice-cold (<4°C) high-sucrose artificial cerebrospinal fluid (aCSF) that contained (in mM): 3 KCl, 2 MgCl₂, 1.25 NaH₂PO₄, 26 NaHCO₃, 10 glucose, 220 sucrose and 2 CaCl₂ (300 mOsm) continuously bubbled with 95% O₂/5% CO₂ (Chen et al. 2009; Sekizawa et al. 2009). Brainstem coronal slices (250 μm thick) containing the intermediate to caudal NTS (0–1,250 μm caudal to obex) were cut with a VT 1000S vibrating microtome (Leica, Richmond, IL, USA). After sectioning, slices were incubated for 45 min at 37°C in high-sucrose aCSF; the slices were placed in normal aCSF at 37°C that contained (in mM): 125 NaCl, 2.5 KCl, 1 MgCl₂,

1.25 NaH₂PO₄, 25 NaHCO₃, 25 glucose and 2 CaCl₂ (300 mOsm) continuously bubbled with 95% O₂/5% CO₂. During the experiments, a single slice was transferred to the recording chamber, held in place with a silk mesh, and continuously perfused with oxygenated aCSF (95% O₂/5% CO₂) at a rate of approximately 4 ml/min.

For temperature control of the oxygenated aCSF in the recording chamber, the perfusion configuration consisted of an inner tube for aCSF delivery to the recording chamber jacketed by an outer tube ~10 cm in length connected at each end to one of three different circulating water baths, each at a fixed temperature. With this concentric tube arrangement placed within 10 cm of the recording chamber, the temperature of aCSF in the recording chamber could be switched to 15, 25, or 33°C while a single slice was submerged and stationary. A temperature probe was placed in the recording chamber to measure aCSF temperature and to ensure slice recordings were within 1°C of one of the three set temperatures.

Neurons were visualized with infrared differential interference contrast imaging, using a charge-coupled device camera (OLY-105, Olympus America Inc., USA) for display on a TV monitor and a video encoding software (Winnov, Sunnyvale, CA, USA) for storage in a PC computer. After establishing a seal with a resistance of >1 GΩ, whole-cell currents or voltages were recorded using borosilicate glass pipettes (3–5 MΩ; 4.0 ± 0.1 MΩ) filled with a potassium gluconate (K-gluconate) based solution containing in (mM): 130 KC₆H₁₁O₇, 1 NaCl, 1 MgCl₂, 2 K-ATP, 0.3 Na-GTP, 10 EGTA and 10 HEPES (300 mOsm); pH was adjusted to 7.4 with KOH at room temperature (22°C). The series resistance was <24 MΩ (13.4 ± 0.8 MΩ). Neither pipette resistance nor series resistance differed between hamster and rat slices (pipette resistance: 3.9 ± 0.1 MΩ and 4.0 ± 0.1 MΩ, respectively; series resistance: 13.9 ± 1.2 MΩ and 12.9 ± 0.9 MΩ, respectively). Recordings were made with the MultiClamp 700B amplifier (Axon Instruments, Foster City, CA, USA). Currents and voltages were filtered at 2 kHz, digitized at 10 kHz with the DigiData1322A interface (Axon Instruments) and stored in an IBM-compatible computer. Data were analyzed off-line using the pCLAMP9.2 software (Axon Instruments) or MiniAnalysis software (Synaptosoft Inc., Decatur, GA, USA).

Identification of second-order NTS neurons

Following establishment of the whole-cell configuration, resting membrane potential, cell capacitance, and input resistance were immediately recorded. A neuron was then tested to ensure that it responded to TS stimulation with its membrane voltage clamped at -60 mV. Those not responding were not used. Stimulating voltages (2–20 V,

0.1 ms square wave pulses) were delivered through bipolar tungsten electrodes (1 μm tips separated by 80 μm, FHC, Bowdoin, ME) to the TS ipsilateral to the recording site with a microelectrode stimulator (SD9; Grass Instruments, Quincy, MA, USA). Using paired-shock stimulation, all neurons included in the study were then confirmed as second-order by two previously established electrophysiological criteria: (1) an excitatory postsynaptic current (EPSC) was consistently evoked by each of two TS stimuli separated by 5 ms (200 Hz), and (2) the variability of the onset latency of the evoked EPSCs was ≤0.5 ms (Miles 1986; Scheuer et al. 1996; Sekizawa et al. 2003).

Classification of action potential firing phenotypes in NTS neurons

Each second-order NTS neuron was further classified as one of two firing phenotypes: RS and DS types (Sekizawa et al. 2009, 2010a, b). Briefly, in current-clamp mode and from a holding membrane potential of -50 mV, the neuron was injected with a hyperpolarizing current to set the membrane potential to -80 mV for 500 ms, followed by a step depolarizing current injection (+100 and +120 pA). A neuron met the first criterion for classification as an RS phenotype if the delay between the onset of the current step and the first action potential (AP) was ≤20 ms (Fig. 1a, left, top trace), while a neuron met the first criterion for classification as a DS type if it responded with significant delay (onset ≥100 ms) (Fig. 1a, right, top trace). To confirm this classification, each neuron was injected with depolarizing current (+100 and +120 pA) without a hyperpolarizing prepulse (Fig. 1a, bottom traces), and the difference in spiking onset in the absence or presence of hyperpolarizing prepulse was calculated. If the calculated difference was ≤10 ms, the neuron met the second criterion for classification as an RS phenotype. If the calculated difference was ≥100 ms, the neuron met the second criterion for classification as a DS type. Neurons in this study were classified as RS or DS phenotypes only if they met both criteria. Figure 1b shows the distribution of calculated spiking onset differences in hamsters and rats. No species differences were observed (Kolmogorov–Smirnov test, $P = 0.913$). Of the 23 NTS neurons (from 9 hamsters), 11 neurons were classified as RS and 12 as DS. Of the 25 NTS neurons (from 7 rats), 12 were classified as RS and 13 as DS. Four neurons from hamsters and two neurons from rats had spiking onsets within the onset range between 20 and 100 ms and were not included in the study. The hyperpolarizing prepulse protocols were only used to classify phenotypes at the beginning of each slice experiment. Thereafter, as described below, intrinsic membrane properties (input resistance, cell capacity, and spiking response to depolarization) were evaluated from a holding potential

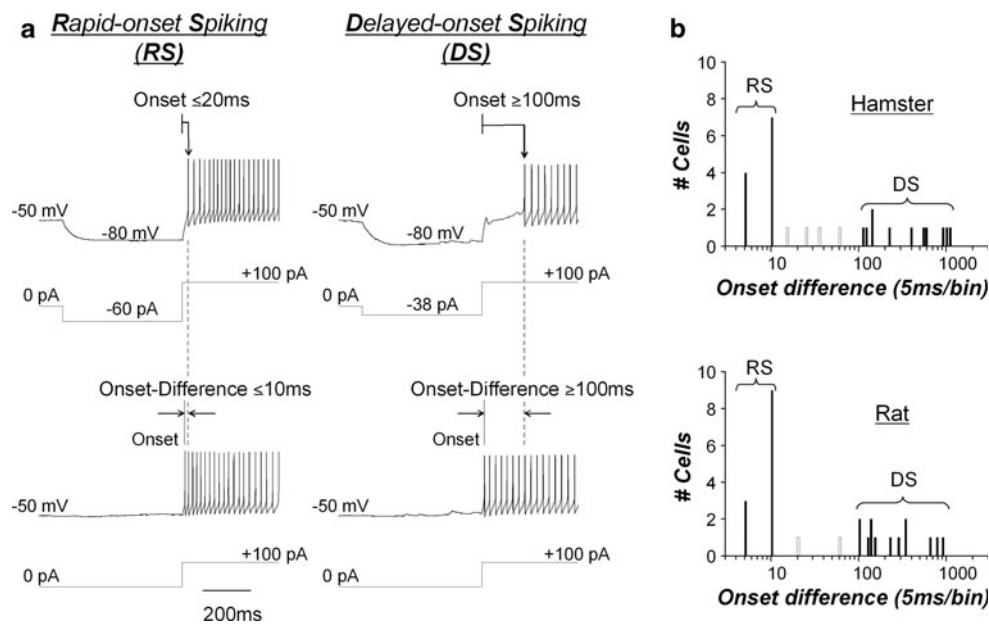


Fig. 1 Classification of a second-order NTS neurons as a RS or DS phenotype. **a** The *top two traces* show action potentials triggered by a depolarizing pulse preceded by a hyperpolarization prepulse. *Left traces* are from a RS neuron and *right traces* are from a DS neuron. Note that the hyperpolarization prepulse causes a ≤ 20 ms delay in the RS neuron and ≥ 100 ms delay in the DS neuron before a train of

action potentials is triggered. The *bottom two traces*, without a prepulse, show trains of action potentials are being immediately triggered by the depolarizing pulse. **b** Histograms of onset difference for neurons in hamsters (*top*) and rats (*bottom*). No significant difference in distribution was observed in these two graphs

of -50 mV, a membrane potential close to their resting membrane potential.

Labeling second-order NTS baroreceptor neurons

In some experiments (3 of the 9 hamsters and 4 of the 7 rats), second-order NTS neurons were further identified as baroreceptor neurons by the fluorescent labeling technique reported previously (Chen et al. 2009; Sekizawa et al. 2009). Briefly, animals were anesthetized by intramuscular injections of ketamine (100 mg kg^{-1} for hamsters and 50 mg kg^{-1} for rats) and xylazine (10 mg kg^{-1} for both hamsters and rats); both aortic depressor nerves were carefully isolated; and a 4–5 mm segment was placed on a section of parafilm for application of the crystal form of the fluorescent tracer, 1,1'-dilinoleyl-3,3,3',3' tetra-methylindocarbocyanine, 4-chlorobenzenesulfonate [FAST DiITM solid; DiI $\Delta^{9,12}\text{-C}_{18}(3)$] on the nerves that were subsequently coated with polyvinylsiloxane gel. To provide time for transport of the dye to the central terminal boutons, the animals were allowed to recover for 2 weeks (Chen et al. 2009; Sekizawa et al. 2009). The fluorescent boutons were visualized with an optical filter set for DiI (U-MWIGA 3, Olympus, Center Valley, PA, USA) and an image integrating system (InstaGater, Dage-MTI, Michigan City, IN, USA). An example of a labeled NTS baroreceptor neuron is shown in Fig. 2.

Protocols

For current-clamp experiments, all neurons were held at -50 mV. With the recording chamber temperature set at 33°C , the input resistance and the whole-cell membrane capacitance were measured by injecting hyperpolarizing currents ($20\text{--}60$ pA, 200 ms). Intrinsic cell excitability was determined by measuring the neuronal spiking response to a 2-s depolarizing current injection (80 pA). When evoked and spontaneous EPSCs were recorded in voltage-clamp experiments, the neuron was held at -60 mV. The evoked EPSCs were generated by TS stimulation at 0.2 Hz. To obtain consistent evoked EPSCs, stimulating voltages were adjusted until maximum EPSC amplitude was elicited in each neuron.

To determine temperature dependency of signal processing in NTS neurons, the slice was then cooled to 25°C by switching the outer tube to a second circulating water bath. After a stable temperature in the recording chamber was reached (~ 5 min after switching), the above protocol for recordings at 33°C was repeated. To complete determination of temperature effects, the aCSF was further cooled to 15°C by switching to a third refrigerated water bath. After approximately 8 min, the temperature of the recording chamber stabilized and the above protocol was repeated. In preliminary experiments, we verified that returning the recording chamber to 33°C (and following the

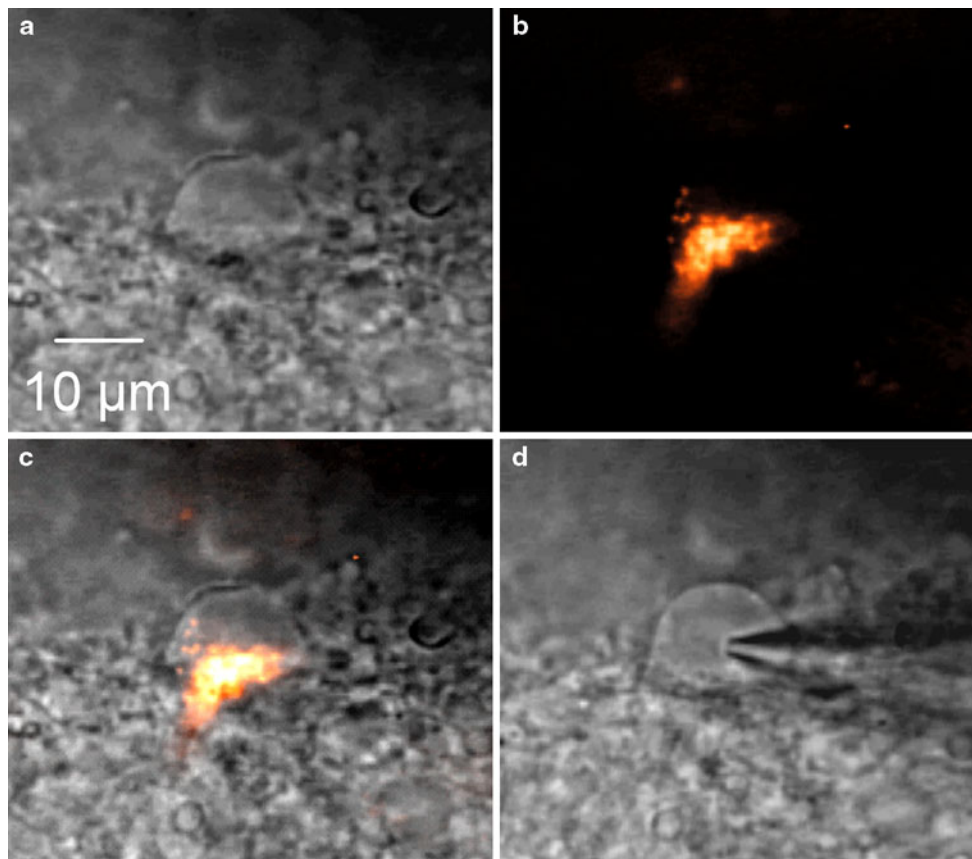


Fig. 2 Anatomical identification of second-order NTS baroreceptor neuron. **a** NTS neuron viewed under infrared differential interference contrast imaging. The scale bar = 10 µm. **b** The same neuron viewed

under fluorescence to visualize presynaptic baroreceptor afferent fiber terminal boutons. **c** Overlay of **a** and **b**. **d** Patch electrode attached to the same cell for whole-cell recording

same protocol initially used at 33°C) reversed changes in firing rates and TS-evoked EPSC waveforms that had been seen upon cooling (data not shown).

Data analysis

The spiking response to the +80 pA depolarizing current pulse was determined by counting the number of spikes. An action potential waveform was characterized by measuring its threshold, width, peak amplitude, and afterhyperpolarization potential. Threshold was measured as the membrane potential where the action potential rose steeply (Nakajima and Onodera 1969), and width was measured at the level of threshold potential. For voltage-clamp experiments, evoked EPSC amplitude, onset latency and rise time (onset to peak) were analyzed. Amplitude and frequency of spontaneous EPSCs were measured over 1-min intervals at each temperature.

Data are expressed as mean \pm standard errors. Resting membrane potential, input resistance, and cell capacitance were analyzed using a two-way ANOVA with animal species (rat vs. hamster) as one factor and neuronal

phenotype (RS vs. DS) as the other factor. Spiking responses, action potential waveforms, evoked EPSC amplitudes and rise times, and spontaneous EPSC amplitudes and frequencies were analyzed with a two-way repeated measures ANOVA with animal species as the between factor and temperature as the within factor. Tukey post hoc test was used for pair-wise comparisons when interaction was significant. For experiments comparing stimulus intensity of TS between rats and hamsters, Student's *t* test was used. Significance was set at $P < 0.05$.

Drugs

Ketamine and xylazine were obtained from Vedco Inc. (St. Joseph, MO, USA); DiI was obtained from Molecular Probes (Eugene, OR, USA); polyvinylsiloxane gel was obtained from Charles Laboratories Inc. (Rockville Center, NY, USA); and K-gluconate, K-ATP, Na-GTP, EGTA, HEPES, and CaCl₂, were obtained from Sigma (St. Louis, MO, USA). All other chemicals were obtained from Fisher (Fair Lawn, NJ, USA).

Results

Intrinsic cell properties of second-order rat and hamster NTS neurons

Three intrinsic properties (resting membrane potential, input resistance, and whole-cell capacitance) were measured at 33°C immediately after formation of the whole-cell configuration (Fig. 3). While the average resting membrane potential of RS neurons was similar in both hamsters and rats (Fig. 3a, -54.4 ± 2.7 and -54.8 ± 3.2 mV, respectively), the resting membrane potential for DS neurons in hamsters (-60.9 ± 2.9 mV) was significantly more hyperpolarized than that in rats (-50.0 ± 2.0 mV). This greater hyperpolarization at near euthermic body temperatures suggests species differences between rat and hamster NTS neurons. However, not all properties showed such differences at 33°C. For example, the input resistance did not differ across all four groups (Fig. 3b). Although the DS neurons are larger than the RS neurons, there was no significant difference between hamsters and rats (Fig. 3c). Taken together, these observations, and additional properties examined below, indicate some, but not all, intrinsic properties of second-order NTS neurons show species differences near the euthermic temperature of rats and hamsters.

For each cell maintained in the whole-cell configuration while slice temperature was decreased from 33 to 25°C and then to 15°C, the spiking response to depolarizing current injection (+80 pA) was measured to determine intrinsic excitability (Fig. 4). As shown in sample traces (Fig. 4a₁, b₁), spiking responses to the depolarizing current injection decreased when temperature dropped from 33 to 15°C, a decrease seen in all NTS neurons. In addition, RS (Fig. 4, left column) and DS (Fig. 4, right column) phenotypes responded differently. Hamster RS neurons had significantly higher spiking rates than did rat RS neurons at all temperatures (Fig. 4a₂). In contrast, the spiking rates of hamster DS and rat DS neurons did not differ with decreased temperature (Fig. 4b₂).

Comparing phenotype responses in each species, we found that spiking responses were significantly greater in hamster RS neurons than in hamster DS neurons (two-way repeated measures ANOVA, RS vs. DS: $P = 0.043$; temperature: $P < 0.001$; interaction: $P = 0.843$). Rat RS and DS neurons had similar firing rates (two-way repeated measures ANOVA, RS vs. DS: $P = 0.475$; temperature: $P < 0.001$; interaction: $P = 0.998$). Thus, hamster RS neurons had the most robust spiking rates of all phenotypes at all three slice temperatures.

Action potentials recorded from a single NTS cell as temperature was decreased exhibited elevated peak amplitudes and marked prolongation in width, but no

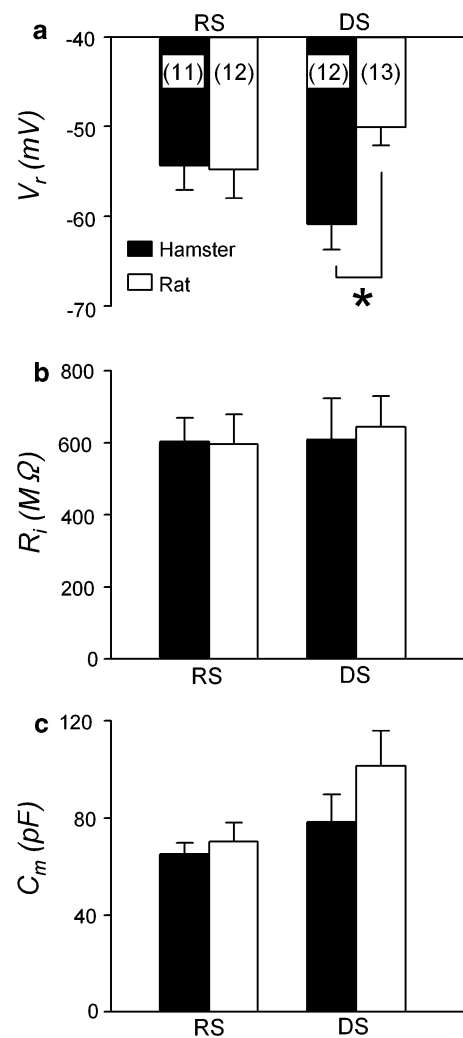


Fig. 3 Resting membrane potential (V_r), input resistance (R_i), and whole-cell capacitance (C_m) at 33°C. **a** V_r of RS neurons in hamsters (filled bar) and rats (open bar) did not differ, but V_r of DS neurons in hamsters was more hyperpolarized than that in rats (two-way ANOVA, $P < 0.05$ for interaction; * $P = 0.006$ within DS neurons). **b** R_i did not differ in either species or neuronal phenotype (two-way ANOVA, $P > 0.05$). **c** The C_m of RS neurons was significantly less than that of DS neurons regardless of the species (two-way ANOVA, $P < 0.05$, RS vs. DS)

significant change in afterhyperpolarization amplitude or AP threshold (Fig. 5a₁, b₁). While all cells exhibited these overall changes in AP waveform, there were specific differences in the responses of hamster versus rat RS and DS phenotypes as well as RS versus DS in the same species. Specifically, RS waveforms (Fig. 5) showed significant species differences in three of four variables. First, AP peak amplitudes in hamsters (66.5 ± 3.4 mV) were significantly smaller than those of rats (77.4 ± 4.9 mV) at 33°C, but were similar at 15°C (Fig. 5a₂). Second, AP widths were significantly prolonged in both species when temperature dropped to 25°C and to 15°C, with those in

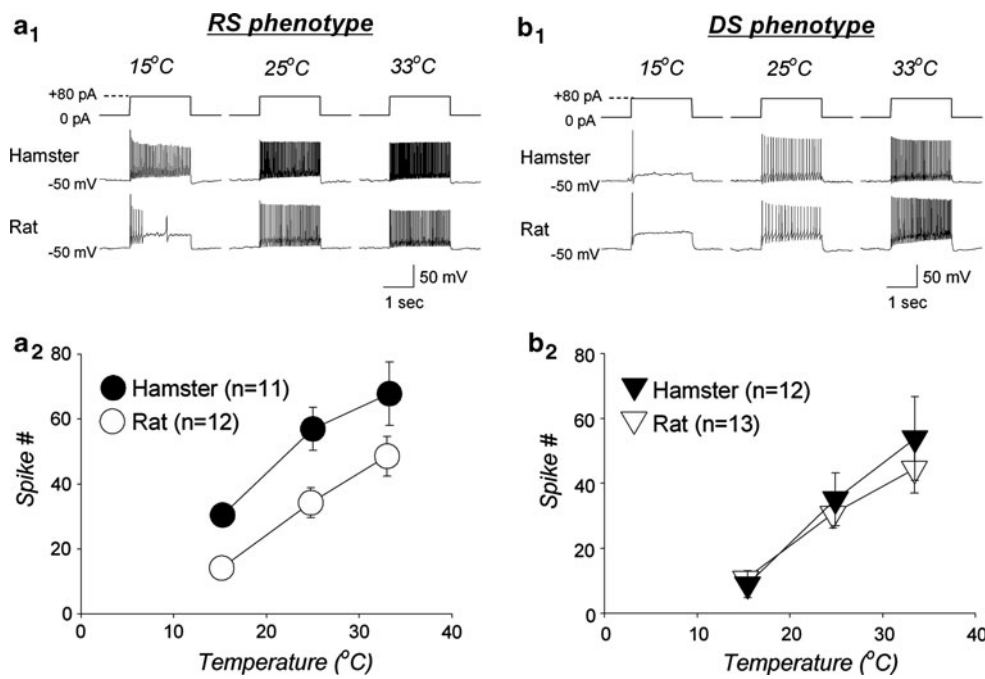


Fig. 4 Spiking responses to depolarization of NTS neurons. **a₁** Spiking responses triggered by current injection in a single hamster RS neuron (**a₁ middle**) and a single rat RS neuron (**a₁ lower**). When temperature dropped from 33°C (*right*) to 15°C (*left*), spiking responses to the same depolarizing current injection were blunted in both species. **a₂** Group data showing significantly higher firing rates in hamster versus rat RS neurons at all three temperatures (two-way repeated measures ANOVA,

$P < 0.05$ for species and temperature). **b₁** Spiking response triggered by current injection in a single hamster DS neuron and a single rat DS neuron demonstrating a decreased spiking response in both species when temperature dropped from 33°C (*right*) to 15°C (*left*). **b₂** Group data showing no differences between hamster and rat DS neurons as both reduced spiking with decreased temperature (two-way repeated measures ANOVA, $P > 0.05$)

hamster neurons (5.9 ± 0.4 ms) being significantly smaller than those in rat neurons (8.4 ± 0.7 ms) at 15°C (Fig. 5a₃), indicating more rapid repolarization. And third, afterhyperpolarization amplitudes were significantly greater in hamster neurons than in those of rats at all temperatures (Fig. 5a₄). In contrast, AP thresholds in hamsters did not statistically differ from those of rats (Fig. 5a₅); and DS waveforms (Fig. 5) showed no significant species differences in any of the four variables with decreased temperature (Fig. 5b₂₋₅) (Table 1).

A comparison of AP widths in RS and DS neurons for each species indicated a significant difference in hamsters (33°C: 1.3 ± 0.1 vs. 1.7 ± 0.1 ms; 25°C: 2.1 ± 0.1 vs. 2.5 ± 0.1 ms; 15°C: 5.9 ± 0.4 vs. 7.6 ± 0.5 ms, respectively), but not in rats (33°C: 1.8 ± 0.1 vs. 1.9 ± 0.2 ms; 25°C: 3.1 ± 0.2 vs. 3.3 ± 0.2 ms; 15°C: 7.8 ± 0.7 vs. 8.8 ± 0.6 ms, respectively) (Table 2). When AP thresholds were compared across all temperatures, RS neurons showed only a “trend” toward a lower threshold in both hamsters and rats (Table 2). The only species difference in AP thresholds that rose to statistical significance was at 15°C where these thresholds were significantly lower in RS than in DS hamster neurons (Table 2). Thus, a major difference in the two phenotypes at low temperatures was that AP waveforms of hamster RS neurons had smaller widths

than did those of hamster DS neurons and rat neurons. These compact APs in hamster RS neurons suggest enhanced temporal fidelity in signal transmission over the axons of this class of gateway neurons.

In a subset of neurons anatomically identified as second-order baroreceptor RS neurons with DiI labeling, the spiking response was also significantly greater in hamsters than in rats (68% higher at 33°C; 95% higher at 25°C; 117% higher at 15°C; two-way repeated measures ANOVA, hamsters vs. rats: $P = 0.048$; temperature: $P < 0.001$; interaction: $P = 0.314$). In addition, AP widths were significantly prolonged in rat neurons compared to hamster neurons as temperature decreased (28% longer at 33°C; 34% longer at 25°C; 54% longer at 15°C; two-way repeated measures ANOVA, hamsters vs. rats: $P = 0.076$; temperature: $P < 0.001$; interaction: $P = 0.046$; Tukey post hoc test: $P = 0.003$ at 15°C). Thus, the second-order neurons receiving baroreceptor inputs had the same properties as did the whole population of second-order neurons.

Synaptic properties of second-order hamster and rat NTS neurons

To evaluate the overall ability of second-order NTS neurons to respond to afferent signals arriving at synapses, we

Fig. 5 Action potential (AP) waveforms. **a₁** Representative traces of an AP waveform from a hamster (*solid line*) and a rat (*dotted line*) RS neuron. **a₂** Group data showing that AP peak amplitude was smaller in hamster RS neurons versus rats at 33°C (two-way repeated measures ANOVA, $P < 0.05$ for temperature and interaction; $*P = 0.049$ at 33°C) and that this difference was abolished at 15°C. **a₃** Group data showing a greater increase in AP width in rat RS neurons as temperature decreased (two-way repeated measures ANOVA, $P < 0.05$ for species, temperature, and interaction; $*P < 0.001$ at 15°C). **a₄** Group data of afterhyperpolarization (AHP) of RS neurons showing no appreciable temperature dependence in either animal species but significantly greater AHPs in hamsters than in rats (two-way repeated measures ANOVA, $P < 0.05$ for species). **a₅** Group data of RS neuronal AP thresholds showing no significant effects of temperature or species (two-way repeated measures ANOVA, $P > 0.05$). **b_{1–5}** AP peak amplitude of both hamster and rat DS neurons increased and AP width was prolonged at 15°C versus 33°C. No significant differences were detected between species in any parameters (statistical results in Table 1)

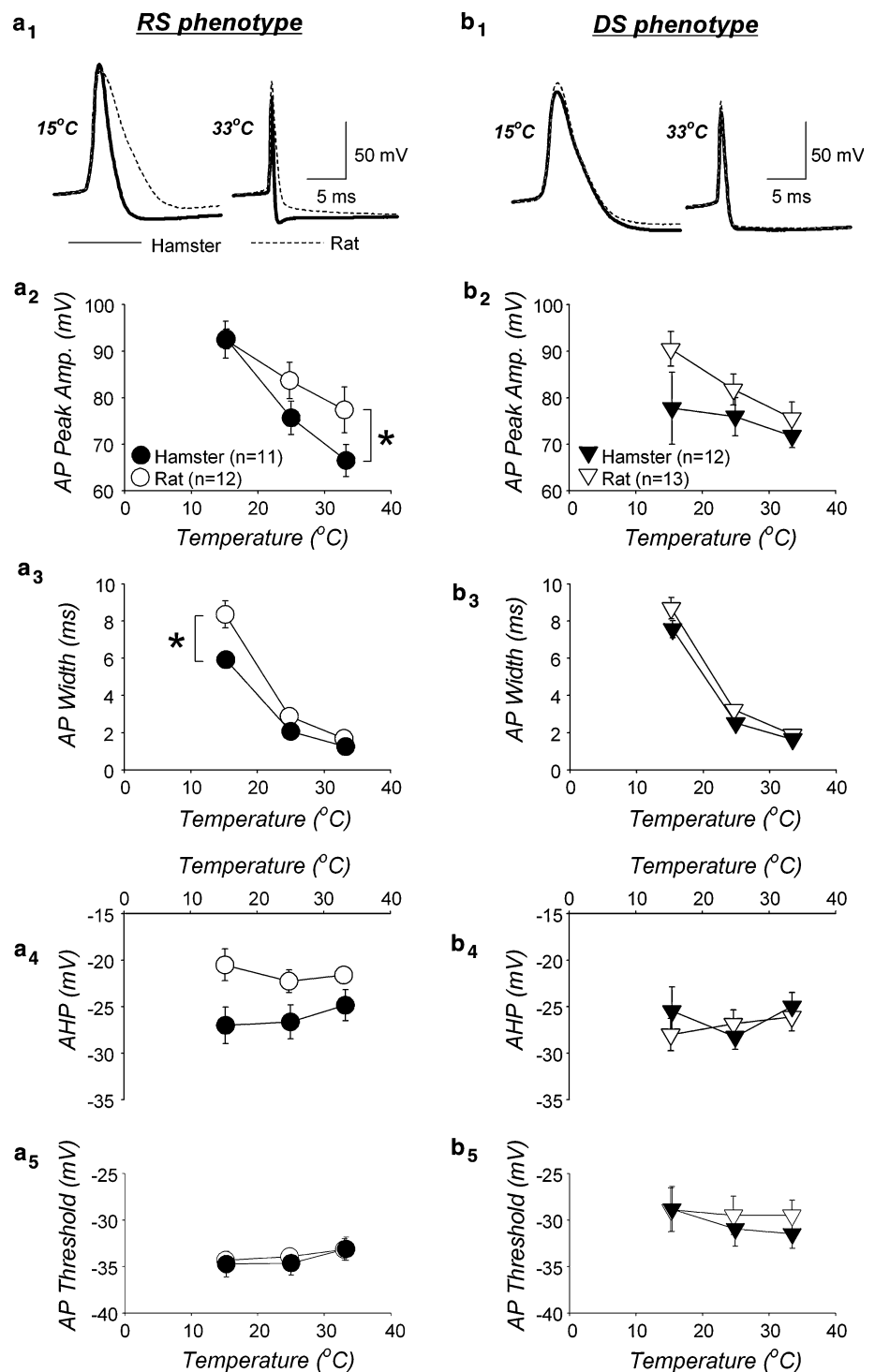


Table 1 ANOVA P values of DS neuronal action potential waveforms

	Hamsters ($n = 12$) vs. rats ($n = 13$)	Temperature	Interaction
AP Peak amplitudes	0.228	<0.001	0.750
AP widths	0.086	<0.001	0.245
Afterhyperpolarization	1.000	<0.001	0.287
AP thresholds	0.818	0.019	0.132

Table 2 ANOVA *P* values for hamster and rat RS and DS neuronal action potential (AP) widths and thresholds

	RS vs. DS	Temperature	Interaction
AP widths in hamsters	0.005	<0.001	0.008
AP widths in rats	0.508	<0.001	0.967
AP thresholds in hamsters	0.064	0.234	0.004
AP thresholds in rats	0.052	0.824	0.377

recorded spontaneous EPSCs (Fig. 6a). The striking decrease in spontaneous EPSCs, recognized as a shrinking event-amplitude distribution in Fig. 6b₁, indicates that as a whole, excitatory synaptic input markedly declined when temperature declined. Significant decreases in spontaneous EPSCs frequency and amplitude occurred as temperature was lowered in both RS (Fig. 6b) and DS (Fig. 6c) neurons. In RS neurons, there was no species difference in spontaneous EPSC frequency (Fig. 6b₂) and amplitude (Fig. 6b₃). In contrast, hamster DS neurons received greater excitatory synaptic inputs as shown by a higher level of spontaneous EPSC frequency (Fig. 6c₂) than did rat DS neurons, while both rat and hamster DS neurons had similar spontaneous EPSC amplitude (Fig. 6c₃).

Compared to hamster RS neurons, hamster DS neurons had a higher spontaneous EPSC frequency (two-way repeated measures ANOVA, RS vs. DS: $P = 0.029$; temperature: $P < 0.001$; interaction: $P = 0.031$) and amplitude (two-way repeated measures ANOVA, RS vs. DS: $P = 0.006$; temperature: $P < 0.001$; interaction: $P = 0.021$). There was no difference in spontaneous EPSC frequency or amplitude between rat RS and rat DS neurons.

To evaluate signal transmission on pathways carrying signals from the periphery to the CNS, we excited first-order fibers by TS stimulation and recorded evoked EPSCs in second-order NTS neurons. When temperature decreased from 33 to 15°C, amplitudes of TS-evoked EPSCs became smaller in all NTS neurons. However, temperature-dependent changes between RS ($n = 11$ – 12) and DS phenotypes ($n = 11$ – 13) within each species were not different, and therefore evoked EPSC data of RS and DS phenotypes were pooled. As seen in example traces of Fig. 7a, evoked EPSCs were greater in a hamster versus a rat neuron at all three experimental temperatures. Group data confirm that evoked EPSC amplitude was significantly larger (>2 fold) in hamsters than rats (Fig. 7b). This larger evoked EPSC amplitude (Fig. 7b) was not the result of a greater stimulus intensity as the averaged stimulus voltage was actually lower in hamsters (hamsters vs. rats: 6.6 ± 0.8 and 10.5 ± 0.9 V, respectively; *t* test: $P = 0.003$). In addition, group data (Fig. 7c) show that the onset latency (the time between the TS stimulus shock artifact and onset of the evoked EPSC in the second-order NTS neuron) at 15°C was

significantly shorter in hamsters (9.2 ± 0.8 ms) than in rats (11.7 ± 0.7 ms). Evoked EPSC rise time was prolonged as temperature dropped, but there was no significant difference between hamsters and rats (two-way repeated measures ANOVA, hamsters vs. rats: $P = 0.097$; temperature: $P < 0.001$; interaction: $P = 0.152$).

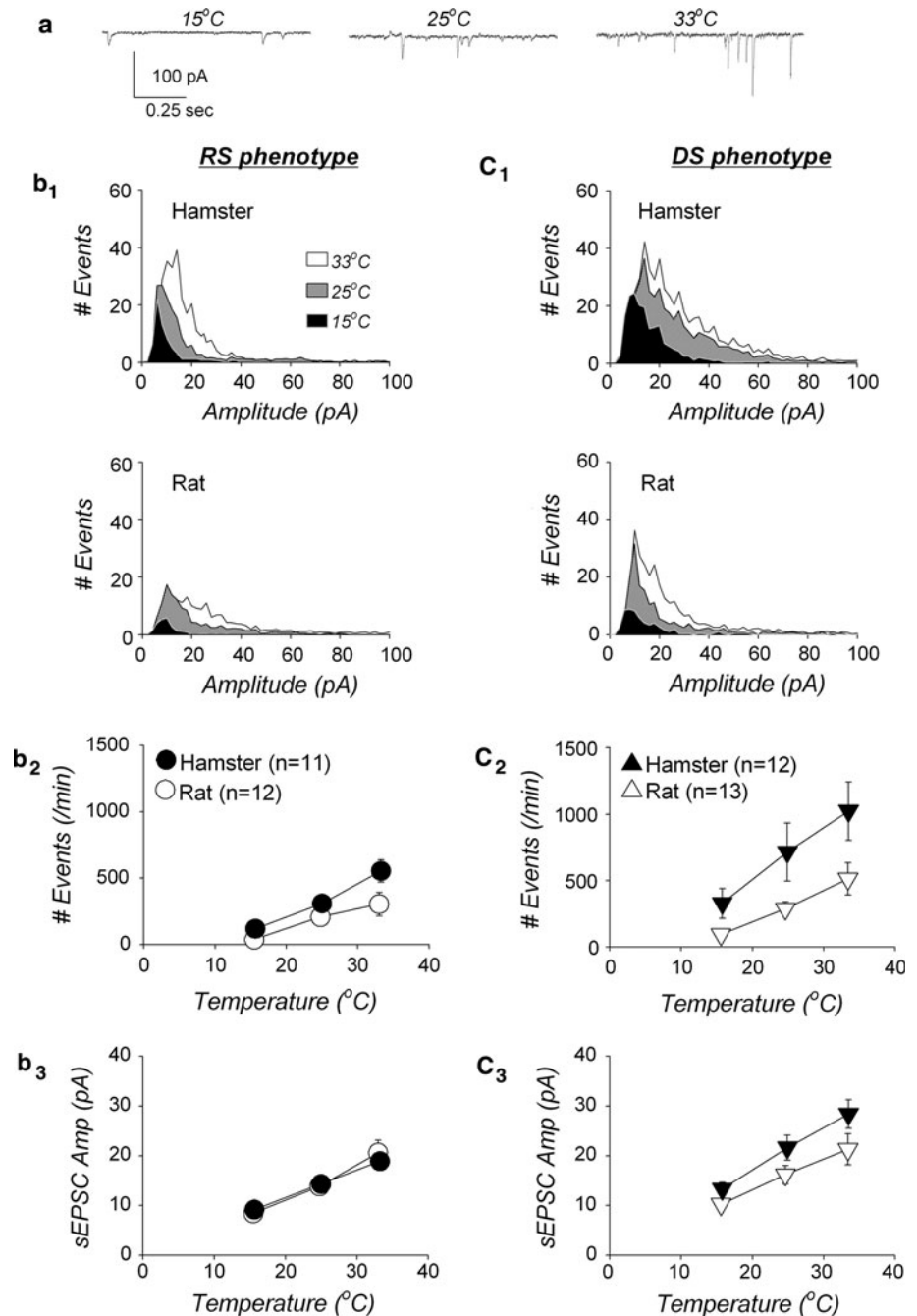
Together, the greater excitatory synaptic inputs from sensory fibers to second-order NTS neurons in the hamster maintain excitability of gateway neurons at low temperatures. In a subset of neurons anatomically identified as second-order baroreceptor neurons by DiI labeling, the evoked EPSC amplitude was also significantly larger in hamsters compared to rats (33°C: 240 ± 61 vs. 110 ± 29 pA; 25°C: 179 ± 45 vs. 84 ± 23 pA; 15°C: 69 ± 15 vs. 21 ± 6.6 pA, two-way repeated measures ANOVA, hamsters vs. rats: $P = 0.032$; temperature: $P < 0.001$; interaction: $P = 0.156$).

Discussion

Our data are consistent with our hypotheses and imply a realignment of signal processing within the NTS as the hamster's brain temperature declines during entry into hibernation. This realignment would allow sensory signals to be reliably processed and relayed to downstream nuclei in central cardiorespiratory circuits with reduced energy expenditure. Both intrinsic and synaptic properties of rat and hamster second-order NTS neurons differ, and Fig. 8 summarizes these species and phenotype differences as well as provides a framework for a detailed discussion of each of the four classes of neurons.

The general effect of lowering temperature from 33°C (Fig. 8 upper row) to 15°C (Fig. 8 lower row) is a marked reduction in both intrinsic and synaptic excitability that is depicted by a shift from red (high activity) to orange (medium activity) and from orange to blue (low activity). The distinctive collection of properties characterizing a phenotype at 33°C was also seen at 25°C and at 15°C with only two exceptions: First, at 15°C, APs over hamster RS neurons were more temporally compact than those of other phenotypes, and second, at 15°C, a shorter delay in TS-stimulated-evoked EPSC onset was recorded in hamster second-order NTS neurons than in those of rats. The general decrease in neural excitability as temperature declined that was observed in all second-order NTS neurons is consistent with electroencephalography and 2-deoxyglucose uptake studies showing reduced CNS activity throughout the brain during entry into hibernation (Chatfield and Lyman 1954; Mihailovic 1972; Kilduff et al. 1982, 1990) and with single unit recordings showing that firing rates of midbrain neurons decreased as the animal naturally entered hibernation (Krilowicz et al. 1989).

Fig. 6 Spontaneous excitatory post-synaptic currents (sEPSCs) **a** Recordings from a single neuron showing that sEPSC frequency was significantly reduced when temperature decreased. **b₁** Average amplitude area plots (2 pA/bin) of sEPSCs in hamster (*upper panel*) and rat (*lower panel*) RS neurons. **b₂** Group data showing that sEPSC frequency was similarly reduced in both species when temperature decreased (two-way repeated measure ANOVA, $P < 0.05$ for temperature). **b₃** Group data showing that sEPSC amplitude was similarly reduced in both species when temperature decreased (two-way repeated measures ANOVA, $P < 0.05$ for temperature). **c₁** Average amplitude area plots of sEPSCs in hamster (*upper panel*) and rat (*lower panel*) DS neurons. **c₂** Group data showing that sEPSC frequency was greater in hamster than rat neurons (two-way repeated measures ANOVA, $P < 0.05$ for species and temperature). **c₃** Group data showing that sEPSC amplitude was reduced to the same degree in both species when temperature decreased (two-way repeated measures ANOVA, $P < 0.05$ for species)



Superimposed on this overall depression in activity are specific species and phenotype differences in second-order NTS neurons. A detailed evaluation of data (see below) shows that at 15°C, a brain temperature encountered during entry into hibernation that is well outside the physiological range of nonhibernators, the remodeled hamster RS phenotype is significantly more excitable than all other hamster and rat phenotypes, despite reduction in its firing rate, implying that this hamster phenotype continues to detect and process sensory signals. In contrast, the remodeled

hamster DS phenotype is silenced to a much greater extent than hamster RS neurons, thus contributing to energy conservation (Fig. 8).

Brain slice studies on signal processing, neuromodulation, and neuroplasticity with the composition of aCSF held constant while temperature is lowered from ~ 30 to $\sim 15^\circ\text{C}$ are considered to be a reasonable model for the temperature effects on the brains of animals entering hibernation (Belousov et al. 1990; Spangenberg et al. 1995; Nikmanesh et al. 1996; Gabriel et al. 1998).

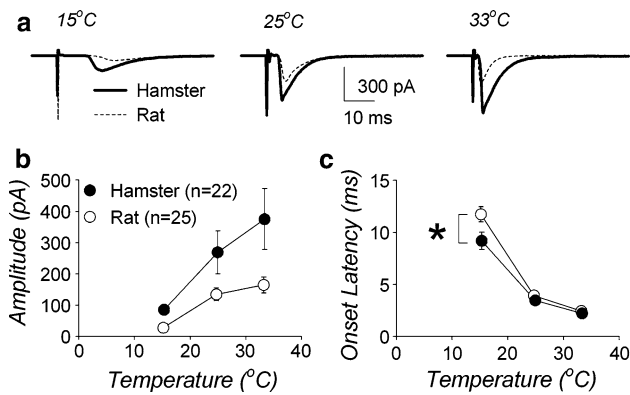


Fig. 7 TS-evoked EPSCs. **a** Sample traces averaged from 10 TS-evoked EPSCs in a hamster neuron and *dotted lines* show evoked EPSCs in a rat neuron. **b** Group data showing that evoked EPSC amplitude was significantly greater in hamsters than in rats (two-way repeated measures ANOVA, $P < 0.05$ for species and temperature). **c** Group data showing that the onset latency was significantly shorter in hamsters at 15°C (two-way repeated measures ANOVA, $P < 0.05$ for temperature and interaction; $*P < 0.001$)

However, this may not be true for slice studies at temperatures below -10°C if aCSF composition is the same as that used at higher temperatures. That is, the aCSF composition may no longer closely approximate in vivo interstitial ionic concentrations since entry into hibernation takes many hours and provides time for regulatory mechanisms to establish new homeostatic states in various compartments. For example, plasma concentrations of K^+ , Mg^{2+} , Ca^{2+} and H^+ have been found to be higher in the hibernating state than in the euthermic state (Igelmund 1995). While the ionic composition of the interstitial compartment bounded by the blood brain barrier may have somewhat similar changes, its composition is not known, and hence cannot be matched by an aCSF in the in vitro slice preparation (Igelmund 1995). Thus, the principal and novel finding of our slice data—that as temperature decreased from 30 to 15°C there was realignment of signal processing—corresponds to changes in brain activity that could occur during *entrance into hibernation*. As is common in slice studies, we speculate that alterations in signal processing established as temperature falls by $\sim 15^{\circ}\text{C}$

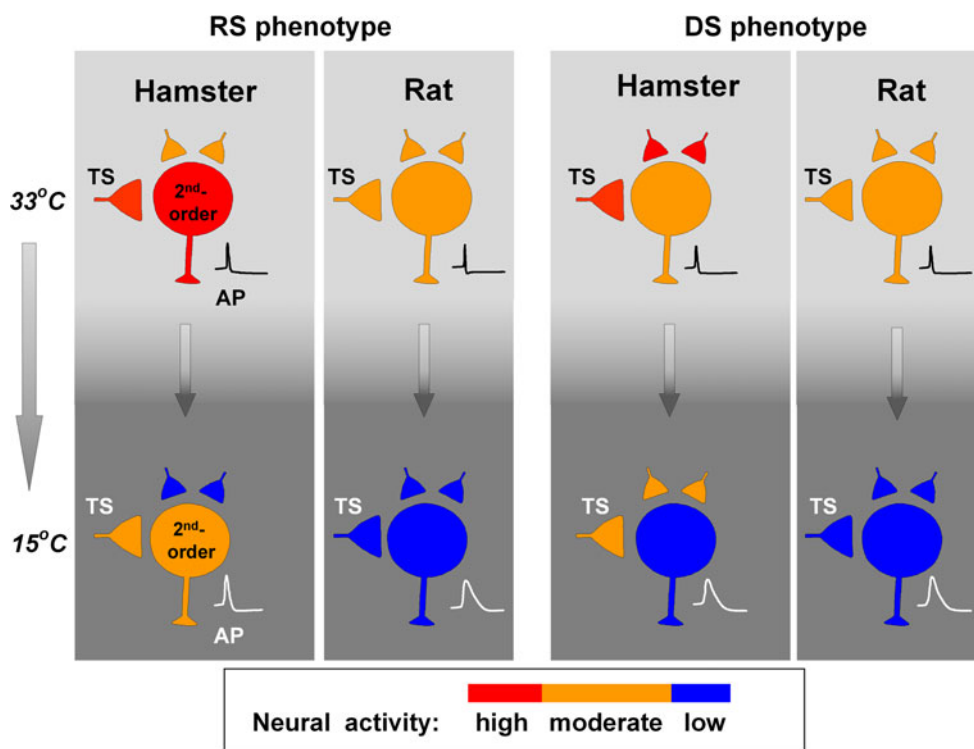


Fig. 8 Comparison of hamster and rat second-order NTS phenotypes. *Upper row* depicts neural activity in 4 phenotypes at 33°C and *lower row* depicts this activity at 15°C . The intensity of synaptic inputs (*triangles*) and the intrinsic excitability of second-order cells (*large circle*) are indicated by the *color scale*. The diagram illustrates three major findings: (1) The RS hamster phenotype (far left column) has the highest electrical activity of all second-order neurons at all temperatures and can contribute to signal transmission over reflex

circuits at both high and low temperatures. At a low temperature (15°C), the APs over the axon of this RS hamster phenotype are still relatively compact, thus preserving signal fidelity. (2) The hamster DS phenotype is moderately active at 33°C and supports signal transmission over reflex arcs, but at 15°C it is much less responsive to inputs and contributes little to signaling over reflex arcs. (3) Overall spontaneous synaptic activity in all phenotypes is greatly attenuated as temperature decreases

persist as brain temperature further decreases and firing rates of neurons throughout the CNS further decline to the low levels of deep hibernation.

Intrinsic excitability of NTS neurons show distinctive species and temperature-dependent differences

The hamster RS neurons had a higher spiking response to a step depolarization than did any other phenotype at all temperatures (Fig. 4). Moreover at 15°C, their APs had a temporally compact waveform (Fig. 5a₁, a₃), suggesting that these neurons can fire at relatively higher frequencies at lower temperature (Wang et al. 2009; Sekizawa et al. 2010a). The compact AP waveform likely improves transmission fidelity by ensuring the brevity of calcium transients and release of transmitters at terminal endings (Wang et al. 2009). These adaptations in the intrinsic excitability of hamster RS neurons make this phenotype stand out at 15°C as more readily generating and propagating compact APs over their axons.

In sharp contrast to the RS neurons, hamster DS neurons were no more excitable than rat DS neurons (Fig. 4b₂), and the AP widths of hamster DS neurons were as broad as those of rat DS neurons (Fig. 5b₃) at lower temperature. Moreover, hamster DS neurons were more hyperpolarized than were rat DS neurons (Fig. 3a), suggesting reduced excitability and degraded temporal fidelity. Previous studies on second-order NTS neurons in the rat showed a more prominent transient outward potassium current in the DS than the RS phenotype (Bailey et al. 2002; Sekizawa et al. 2010a). In the hamster DS phenotype, a hyperpolarization prepulse also removed potassium channel inactivation, thereby allowing activation of many potassium channels by a depolarizing pulse to delay the triggering of a train of APs by ≥ 100 ms (Fig. 1). This suggests that adaptations tending to arrest hamster DS neuronal excitability are present in a phenotype that already had prominent potassium channel currents in both rats and hamsters.

The finding that AP peak amplitudes in all neurons increased when temperature decreased from 33 to 15°C (Fig. 5a₂, 5b₂), is consistent with the observation in a variety of neurons that such peak amplitudes increase or remain high over this range of temperatures (Hodgkin and Katz 1949; Russ and Siemen 1996). Thus, there is no failure in the ability of the NTS phenotypes to generate action potentials at low temperatures. However, the higher AP amplitude in the hamster RS neurons compared to that of their DS neurons supports the importance of RS neurons in signal transmission and that of DS neurons in conserving energy during hibernation.

Taken as a whole, data in Figs. 3, 4 and 5 show that adaptations in all intrinsic properties act together to remodel each phenotype in a distinctive manner. These

intrinsic adaptations are localized to neurons within the NTS and indicate that phenotypes within one brainstem nucleus can exhibit a distinctively different but coherent set of adaptations.

Synaptic excitability of NTS neurons show distinctive species and temperature-dependent differences

While the measured spontaneous EPSCs reflect spontaneous transmitter release from fibers terminating on NTS neurons (Fig. 6), TS stimulation-evoked activity, evoked EPSCs (Fig. 7), reflects inputs from just the peripheral sensory afferents. The evoked EPSCs of gateway hamster NTS neurons to sensory afferent inputs mark the first stage in processing signals that are subsequently relayed to downstream nuclei to maintain cardiorespiratory reflex signaling. Although evoked EPSCs showed species differences, synaptic responses in RS and DS phenotypes did not differ within each species (Fig. 7).

The TS-evoked EPSCs in second-order NTS neurons were significantly greater in hamsters than in rats. Because our noise analysis suggests that single glutamate receptor conductance is similar in hamsters and rats (Supplemental Fig. 1), we have interpreted the evoked EPSC data as supporting the view that more glutamate receptors are activated in the hamster than in the rat. A number of factors may contribute to the greater evoked EPSCs in hamsters, including increased synaptic glutamate release from terminal endings, greater number of afferents being activated, more terminals innervating the postsynaptic neurons, and/or increased postsynaptic receptors. In this regard, Zhang et al. (2009) showed that rats exposed to chronic sustained hypoxia also had greater evoked EPSC amplitudes, an increased responsiveness they attributed to presynaptic mechanisms causing increased glutamate release and a postsynaptic increase in AMPA receptor expression (Zhang et al. 2009). However, further experiments are needed to determine the underlying mechanism(s) mediating enhanced signal transmission in hamsters. Because the amplitude of spontaneous EPSCs was similar between rats and hamsters, the data also suggest that synaptic adaptations are mostly limited to the connections between primary afferents and second-order NTS neurons. Regardless of the mechanism(s), our data are consistent with hamster gateway neurons being more responsive to sensory inputs, facilitating retention of hamster NTS operation at low brain temperatures.

While at all temperatures spontaneous EPSCs were higher in hamster DS neurons than in other phenotypes (Fig. 6c), DS neurons in both species exhibited a major reduction in spontaneous activity with falling temperature (Figs. 6, 8). This reduction is consistent with the overall decrease in CNS activity observed as animals enter

hibernation (Chatfield and Lyman 1954; Mihailovic 1972; Kilduff et al. 1982, 1990). The falloff in spontaneous EPSCs with declining temperature implies decreased activity, including modulatory inputs. Silencing modulatory inputs to NTS neurons during hibernation may have the advantage of eliminating nonessential activity while maintaining the fidelity of essential signals from sensory afferents.

Functional hamster NTS phenotype remodeling

Taken together, our data indicate that synaptic and intrinsic properties for each hamster phenotype combine to functionally remodel the neuron at low temperatures and thus modify overall NTS energy conservation, neuroprotection and neurocontroller operation. That evoked EPSC amplitudes did not significantly differ in hamster RS and DS phenotypes at 15°C implies that glutamatergic receptors on both gateway NTS phenotypes in the hamster were equally responsive to sensory inputs. In contrast to this similarity in synaptic processing (Fig. 8, orange triangles), the intrinsic properties of the RS phenotype acted in concert to sustain electrical excitability (Fig. 8, orange cell body) while the DS phenotype was much less responsive (Fig. 8, blue cell body). Thus, hamster RS neurons are remodeled and sustain signal transmission at low temperatures while hamster DS neurons are not.

When RS and DS neurons were held at same membrane potential, hamster DS neurons had higher spontaneous EPSC frequencies compared to those of rat DS neurons. This suggests that the hamster DS neurons retain their ability to respond to sensory inputs at lower temperatures. However, *in vivo*, these signals are likely to be muted because these DS neurons have a more hyperpolarized membrane potential than do rat DS neurons.

We have interpreted the differences in rat versus hamster data in this study as adaptations in the Syrian hamster that facilitate maintenance of NTS signal processing during entrance into hibernation, although additional factors such as age may have contributed in part to these species differences. For example, the rats in this study were young adults, in the age range of those used in a study showing that NTS neurons from young adult rats (3–5 months old) had similar intrinsic membrane properties to those of older adults (10–12 months old), including resting membrane potential, membrane time constant, action potential waveform, and firing properties (Johnson and Felder 1993). Our hamsters, while not age matched to the rats, were in the age range where the rat NTS had stable properties. Thus, while age difference may be a contributing factor to the differences we saw between the hamsters and rats in this study, any contribution is likely to be small in light of the stability of intrinsic neuron properties described by Johnson and Felder. Another possible contributing factor to the

differences we report may be due to species variations that are independent of the ability to hibernate. However, the following two facts support the view that the major contributor to the differences we saw in this study arose because the hamster is a hibernator and the rat is not: (1) the amplitudes of TS-evoked EPSCs in the NTS at 33°C are similar between rats, guinea pigs, and rhesus monkeys (all nonhibernators) while evoked EPSCs in the hamsters were significantly larger (Sekizawa et al. 2008; Sekizawa et al. 2010b); and (2) neurons in the medial septum-diagonal band complex of the Yakutian ground squirrel (*Citellus undulatus*), a hibernating species, have firing rates approximately twice that of corresponding neurons in the guinea pig, and these ground squirrel neurons have been postulated to actively participate in terminating a hibernation bout to ensure full arousal (Belousov et al. 1990). Our study plus that of Belousov et al. (1990) indicate that electrical excitability is enhanced in at least two subcortical neural populations in hibernating species. Finally, Igelmund (1995) suggested that adaptations that increased neuronal excitability in selected neural populations crucial to sustained signal processing at low temperatures compensate for the general slowing of neural activity in all neurons at declining temperature. The enhanced excitability of RS neurons that we observed in the hamster NTS is consistent with Igelmund's suggestion because the NTS is a component of cardiorespiratory reflexes that *match* oxygen delivery to oxygen demand at all stages of a hibernation bout, including deep hibernation and arousal. Taken together, it appears likely that differences in rat and hamster NTS properties observed in this study can largely be attributed to adaptations in the hamster supporting signal processing at low temperatures.

Fundamental adaptations that conserve energy (Carey et al. 2003) include lowering the thermocontroller setpoint during entry into torpor and continual regulation of T_{core} throughout the torpor bout (Florant and Heller 1977; Heller 1979). Not only is metabolic rate reduced during hibernation as a result of the physical effects of temperature on chemical reactions, but additional savings are achieved by physiological changes in numerous organ systems including the CNS. That the brain of euthermic ($T_{\text{core}} = \sim 37^{\circ}\text{C}$) mammals has a relatively high energy need, accounting for as much as $\sim 20\%$ of the animal's resting metabolism (Rolfe and Brown 1997), and action potentials account for 47% of the neurons' energy expenditure (Attwell and Laughlin 2001) indicate substantial energy savings can be achieved through reduction of neuronal activity. Our data not only show that identified RS and DS phenotypes have lower intrinsic firing rates at 15°C than at 33°C, but also the novel observation that at low temperatures hamster DS neurons have adaptations that further suppress their electrical activity while activity in hamster RS neurons is

maintained at levels sufficient to support signal transmission (Fig. 4). In the hamster NTS, augmented energy savings are achieved in part by intrinsic adaptations that hyperpolarize the DS phenotype (Fig. 3), placing the resting membrane potential closer to the K^+ equilibrium potential so that less energy must be expended by the Na^+/K^+ membrane pump to maintain the K^+ transmembrane gradient. Thus, even within a brainstem nucleus that must continue to operate over a hibernation bout, DS neurons are silenced to save energy while RS neurons “take over” to maintain signal transmission.

Neuroprotective adaptations, many on the apoptotic pathway, also enhance anoxic tolerance in hibernating species (Drew et al. 2001, 2004), resulting in prevention of damage that could disable neurocontrollers. The silenced DS neurons may contribute to anoxic tolerance by reducing the oxygen needed by the CNS and thus extending the margin of safe cardiorespiratory controller operation.

NTS adaptations also fit well within the framework of functional remodeling that successively places many brain regions in a “standby” state during entrance into torpor, an orderly stepwise process reversed during arousal. Neurons in standby mode retain their viability but contribute little to neural processing. For example, averaged auditory-evoked potentials in response to 60 db clicks that result in compact responses in brainstem nuclei in euthermic ground squirrels (*S. lateralis*) failed to evoke such responses when T_{core} fell to 10°C (Horowitz and Horrigan 1996). Nonetheless, during torpor, neurons along the chain of nuclei on the auditory pathway to the neocortex are not totally unexcitable as evidenced by the fact that loud tapping evoked a cortical-evoked response in an otherwise flat electroencephalography (Strumwasser 1959). During entrance into hibernation, many neurons, beginning with neocortical cells, appear to enter this standby energy conserving state, as shown by the successive flattening of electroencephalography activity in cortical structures (Chatfield and Lyman 1954; Mihailovic 1972). In fact, decorticate and decerebellar marmots can still enter hibernation, a finding that has focused attention on subcortical regions, particularly the hypothalamus and brainstem, whose continued operation is essential for survival (see Satinoff 1978). Data on NTS neurons (Fig. 4) are consistent with this general pattern and extend it to a finer level of organization by demonstrating that within a single brainstem nucleus, one NTS phenotype (the hamster DS neuron) can be placed in a standby mode while a second (the hamster RS neuron) sustains reflex operation.

Functional remodeling is not limited to CNS neurons being in standby mode; it also equips neurocontrollers in hibernating species with features not seen in nonhibernating species. With reset setpoints, controllers in hibernating

species maintain a well-regulated internal environment in torpor that is quite different from their euthermic state (Malan et al. 1973; Florant and Heller 1977; Heller 1979). In addition, hibernators have the remarkable capacity to coordinate activation of effectors in an orderly series of events during arousal. These events begin with increased respiratory rates which blow off CO_2 (Malan et al. 1973); They are followed by activation of nonshivering thermogenesis via a chain of subcortical networks (Morrison et al. 2008) to convert chemical energy in brown adipose tissue to heat, rewarm the core and brain of the animal (Smith and Horwitz 1969), and subsequently, by increasing blood flow to the periphery and activation of shivering, complete the rewarming/arousal of the animal (Horwitz et al. 1968). This sequence of steps is controlled by adaptations in subcortical nuclei of hibernating species, and our studies indicate that signals over RS neurons in the NTS remain excitable and responsive to TS inputs and hence can participate in this orderly activation.

In conclusion, our data show that adaptations in synaptic and intrinsic properties of two second-order hamster NTS gateway phenotypes were not identical, with each phenotype being remodeled in a different fashion. Additional studies are required to determine if the finding of major phenotype differences in the NTS gateway neurons can be generalized to higher order hamster NTS neurons and even more broadly generalized to other brainstem nuclei. The substantial drop in spontaneous activity shown by the shrinking area under the curve as temperature falls (Fig. 6) in second-order NTS neurons raises the question of other brainstem neurons also being stripped of “unnecessary” inputs. Moreover, the recent observation that some NTS neurons excited by monosynaptic TS stimulation send their axons directly to a downstream nucleus important for cardiorespiratory reflexes, the rostral ventrolateral medulla (Kline et al. 2010), invites speculation that overall NTS remodeling at low brain temperatures may lead to a stripped down circuit centered on RS neurons that relay temporally compact APs directly to downstream nuclei, a hypothesis that needs testing. Data in the current study centered solely on gateway NTS neurons and demonstrated that hamster phenotypes have distinctive adaptations that contribute to energy conservation, neuroprotection, and functional remodeling that likely contribute to survival during hibernation.

Acknowledgments This study was supported by NIH (R01 HL091763). The breeders of our colony of hamsters used in this study were generous gifts from Dr. John R. Willis at the University of Illinois. The authors thank Jock Hamilton and Sat Chau for critical proofreading. All protocols were approved by the UC Davis Institutional Animal Care and Use Committee in compliance with the Animal Welfare Act and Public Health Service Policy on Humane Care and Use of Laboratory Animals.

References

- Attwell D, Laughlin SB (2001) An energy budget for signaling in the grey matter of the brain. *J Cereb Blood Flow Metab* 21:1133–1145. doi:10.1097/00004647-200110000-00001
- Bailey TW, Jin YH, Doyle MW, Andresen MC (2002) Vanilloid-sensitive afferents activate neurons with prominent A-type potassium currents in nucleus tractus solitarius. *J Neurosci* 22:8230–8237. 22/18/8230 [pii]
- Belousov AB, Vinogradova OS, Pakhotin PI (1990) Paradoxical state-dependent excitability of the medial septal neurons in brain slices of ground squirrel, *Citellus undulatus*. *Neuroscience* 38:599–608. 0306-4522(90)90054-8 [pii]
- Bonham AC, Chen CY, Sekizawa S, Joad JP (2006) Plasticity in the nucleus tractus solitarius and its influence on lung and airway reflexes. *J Appl Physiol* 101:322–327. doi:10.1152/jappphysiol.00143.2006
- Carey HV, Andrews MT, Martin SL (2003) Mammalian hibernation: cellular and molecular responses to depressed metabolism and low temperature. *Physiol Rev* 83:1153–1181. doi:10.1152/physrev.00008.2003
- Chatfield PO, Lyman CP (1954) Subcortical electrical activity in the golden hamster during arousal from hibernation. *Electroencephalogr Clin Neurophysiol* 6:403–408
- Chen CY, Bechtold AG, Tabor J, Bonham AC (2009) Exercise reduces GABA synaptic input onto nucleus tractus solitarii baroreceptor second-order neurons via NK1 receptor internalization in spontaneously hypertensive rats. *J Neurosci* 29:2754–2761. doi:10.1523/JNEUROSCI.4413-08.2009
- Drew KL, Rice ME, Kuhn TB, Smith MA (2001) Neuroprotective adaptations in hibernation: therapeutic implications for ischemia-reperfusion, traumatic brain injury and neurodegenerative diseases. *Free Radic Biol Med* 31:563–573. S0891584901006281 [pii]
- Drew KL, Harris MB, LaManna JC, Smith MA, Zhu XW, Ma YL (2004) Hypoxia tolerance in mammalian heterotherms. *J Exp Biol* 207:3155–3162. doi:10.1242/jeb.01114
- Florant GL, Heller HC (1977) CNS regulation of body temperature in euthermic and hibernating marmots (*Marmota flaviventris*). *Am J Physiol* 232:R203–R208
- Gabriel A, Klusmann FW, Igelmund P (1998) Rapid temperature changes induce adenosine-mediated depression of synaptic transmission in hippocampal slices from rats (non-hibernators) but not in slices from golden hamsters (hibernators). *Neuroscience* 86:67–77. S0306-4522(98)00011-6 [pii]
- Heller HC (1979) Hibernation: neural aspects. *Annu Rev Physiol* 41:305–321. doi:10.1146/annurev.ph.41.030179.001513
- Hodgkin AL, Katz B (1949) The effect of temperature on the electrical activity of the giant axon of the squid. *J Physiol* 109:240–249
- Horowitz JM, Horrigan DJ (1996) Hibernation in mammals: central nervous system functions. In: Fregly MJ, Blatteis CM (eds) *Handbook of physiology*. Oxford University Press, New York, pp 533–539
- Horwitz BA, Smith RE, Pengelley ET (1968) Estimated heat contribution of brown fat in arousing ground squirrels (*Citellus lateralis*). *Am J Physiol* 214:115–121
- Igelmund P (1995) Modulation of synaptic transmission at low temperatures by hibernation-related changes in ionic microenvironment in hippocampal slices of golden hamsters. *Cryobiology* 32:334–343. doi:10.1006/cryo.1995.1034
- Joad JP, Sekizawa S, Chen CY, Bonham AC (2007) Air pollutants and cough. *Pulm Pharmacol Ther* 20:347–354. doi:10.1016/j.pupt.2006.10.013
- Johnson SM, Felder RB (1993) Effects of aging on the intrinsic membrane properties of medial NTS neurons of Fischer-344 rats. *J Neurophysiol* 70:1975–1987
- Kilduff TS, Sharp FR, Heller HC (1982) [¹⁴C]2-deoxyglucose uptake in ground squirrel brain during hibernation. *J Neurosci* 2:143–157
- Kilduff TS, Miller JD, Radeke CM, Sharp FR, Heller HC (1990) 14C-2-deoxyglucose uptake in the ground squirrel brain during entrance to and arousal from hibernation. *J Neurosci* 10:2463–2475
- Kline DD, King TL, Austgen JR, Heesch CM, Hasser EM (2010) Sensory afferent and hypoxia-mediated activation of nucleus tractus solitarius neurons that project to the rostral ventrolateral medulla. *Neuroscience* 167:510–527. doi:10.1016/j.neuroscience.2010.02.012
- Krilowicz BL, Edgar DM, Heller HC (1989) Action potential duration increases as body temperature decreases during hibernation. *Brain Res* 498:73–80
- Malan A, Arens H, Waechter A (1973) Pulmonary respiration and acid-base state in hibernating marmots and hamsters. *Respir Physiol* 17:45–61
- Mihailovic LT (1972) Cortical and subcortical electrical activity in hibernation and hypothermia. In: South FE, Hannon J, Willis JR, Pengelley ET, Alpert NR (eds) *Hibernation and hypothermia, perspectives and challenges*. Elsevier, Amsterdam, pp 487–533
- Miles R (1986) Frequency dependence of synaptic transmission in nucleus of the solitary tract in vitro. *J Neurophysiol* 55:1076–1090
- Morrison SF, Nakamura K, Madden CJ (2008) Central control of thermogenesis in mammals. *Exp Physiol* 93:773–797. doi:10.1113/expphysiol.2007.041848
- Nakajima S, Onodera K (1969) Membrane properties of the stretch receptor neurones of crayfish with particular reference to mechanisms of sensory adaptation. *J Physiol* 200:161–185
- Nikmanesh FG, Spangenberg H, Igelmund P (1996) Histamine enhances synaptic transmission in hippocampal slices from hibernating and warm-acclimated Turkish hamsters. *Neurosci Lett* 210:119–120. 0304394096126720 [pii]
- Rolfé DF, Brown GC (1997) Cellular energy utilization and molecular origin of standard metabolic rate in mammals. *Physiol Rev* 77:731–758
- Russ U, Siemen D (1996) Kinetic parameters of the ionic currents in myelinated axons: characterization of temperature effects in a hibernator and a nonhibernator. *Pflügers Arch* 431:888–894
- Satinoff E (1978) Neural organization and evolution of thermal regulation in mammals. *Science* 201:16–22
- Scheuer DA, Zhang J, Toney GM, Mifflin SW (1996) Temporal processing of aortic nerve evoked activity in the nucleus of the solitary tract. *J Neurophysiol* 76:3750–3757
- Sekizawa S, Joad JP, Bonham AC (2003) Substance P presynaptically depresses the transmission of sensory input to bronchopulmonary neurons in the guinea pig nucleus tractus solitarius. *J Physiol* 552:547–559. doi:10.1113/jphysiol.2003.051326
- Sekizawa S, Chen CY, Bechtold AG, Tabor JM, Bric JM, Pinkerton KE, Joad JP, Bonham AC (2008) Extended secondhand tobacco smoke exposure induces plasticity in nucleus tractus solitarius second-order lung afferent neurons in young guinea pigs. *Eur J Neurosci* 28:771–781. doi:10.1111/j.1460-9568.2008.06378.x
- Sekizawa S, Bechtold AG, Tham RC, Bonham AC (2009) A novel postsynaptic group II metabotropic glutamate receptor role in modulating baroreceptor signal transmission. *J Neurosci* 29:11807–11816. doi:10.1523/JNEUROSCI.2617-09.2009
- Sekizawa S, Joad JP, Pinkerton KE, Bonham AC (2010a) Secondhand smoke exposure alters K⁺ channel function and intrinsic cell excitability in a subset of second-order airway neurons in the nucleus tractus solitarius of young guinea pigs. *Eur J Neurosci* 31:673–684. doi:10.1111/j.1460-9568.2010.07093.x
- Sekizawa S, Joad JP, Pinkerton KE, Bonham AC (2010b) Secondhand tobacco smoke exposure differentially alters nucleus tractus solitarius neurons at two different ages in developing non-human

- primates. *Toxicol Appl Pharmacol* 242:199–208. doi:[10.1016/j.taap.2009.10.009](https://doi.org/10.1016/j.taap.2009.10.009)
- Smith RE, Horwitz BA (1969) Brown fat and thermogenesis. *Physiol Rev* 49:330–425
- Spangenberg H, Nikmanesh FG, Igelmund P (1995) Long-term potentiation at low temperature is stronger in hippocampal slices from hibernating Turkish hamsters compared to warm-acclimated hamsters and rats. *Neurosci Lett* 194:127–129
- Strumwasser F (1959) Regulatory mechanisms, brain activity and behavior during deep hibernation in the squirrel, *Citellus beecheyi*. *Am J Physiol* 196:23–30
- Taylor EW, Jordan D, Coote JH (1999) Central control of the cardiovascular and respiratory systems and their interactions in vertebrates. *Physiol Rev* 79:855–916
- Wang LY, Fedchyshyn MJ, Yang YM (2009) Action potential evoked transmitter release in central synapses: insights from the developing calyx of Held. *Mol Brain* 2:36. doi:[10.1186/1756-6606-2-36](https://doi.org/10.1186/1756-6606-2-36)
- Zhang W, Carreno FR, Cunningham JT, Mifflin SW (2009) Chronic sustained hypoxia enhances both evoked EPSCs and norepinephrine inhibition of glutamatergic afferent inputs in the nucleus of the solitary tract. *J Neurosci* 29:3093–3102. doi:[10.1523/JNEUROSCI.2648-08.2009](https://doi.org/10.1523/JNEUROSCI.2648-08.2009)